Supplemental material

Hartweger et al., https://doi.org/10.1084/jem.20190287

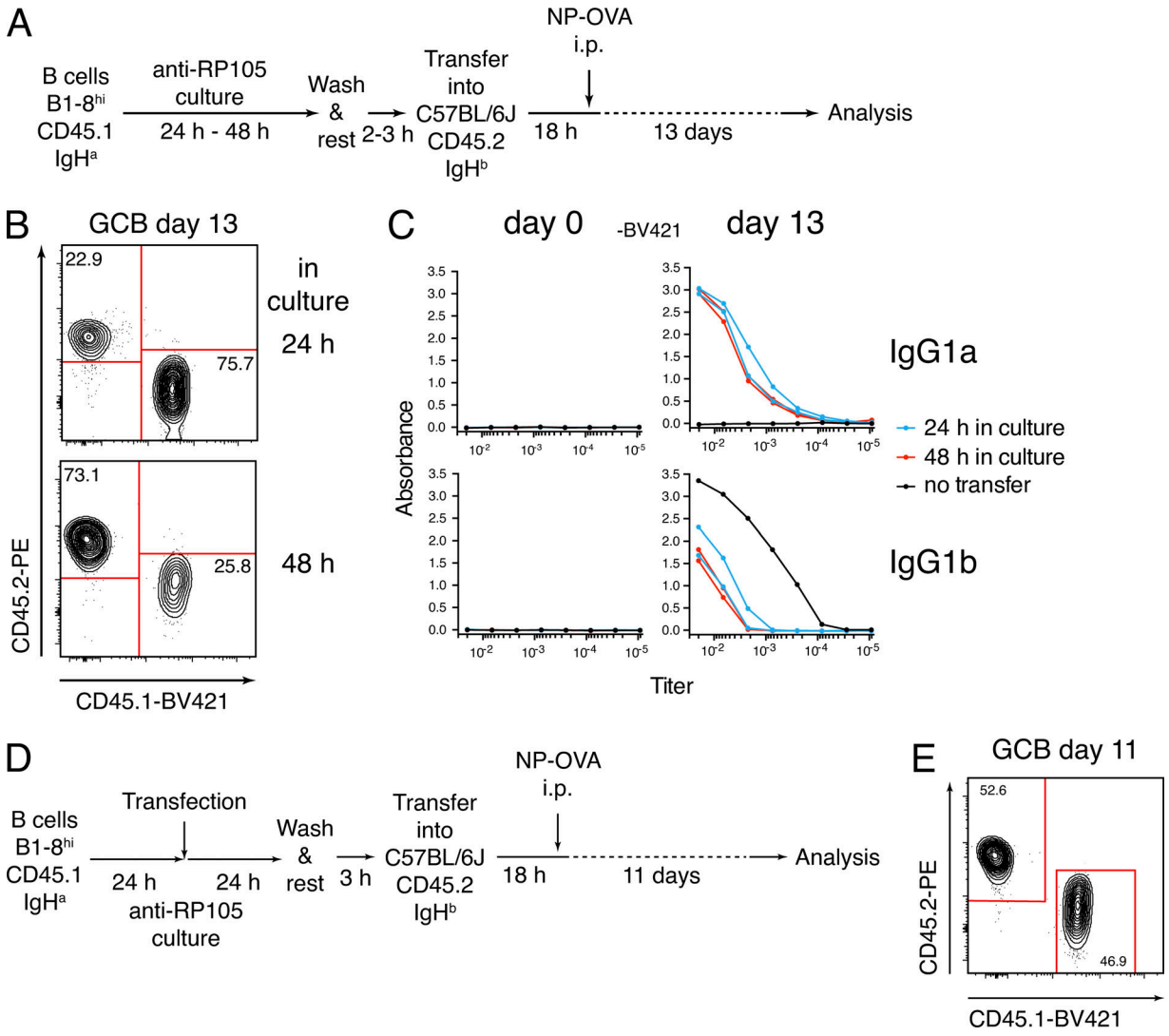

Figure S1. **Cultured B cells participate in humoral immune responses. (A)** Schematic representation of the experimental setup for B and C. B1-8^{hi} CD45.1 Igh^{a} cells were cultured for 24 or 48 h in the presence of anti-RP105 antibody, then rested for 2–3 h without antibody and then transferred into C57BL6/J (CD45.2 Igh^{b}) recipients. 18 h later, mice were immunized with NP-OVA i.p., and mice were analyzed 2 wk later. **(B)** Flow-cytometric plots gated on CD38^{-}Fas^{+}GL7^{+}IgD^{-} GC B cells 2 wk after transfer. **(C)** Pre-immune (day 0) and day 13 ELISA titers of anti-NP IgG1^{a} or IgG1^{b}. **(D)** Schematic representation of the experimental setup for E. B1-8^{hi} CD45.1 Igh^{a} cells were cultured for 24 h and transfected with plasmid DNA. 24 h after transfection cells were transferred and analyzed as in A. **(E)** Flow-cytometric plots gated on CD38^{-}Fas^{+}GL7^{+}IgD^{-} GC B cells 11 d after transfer. Data (A–E) are representative of two or three independent experiments.

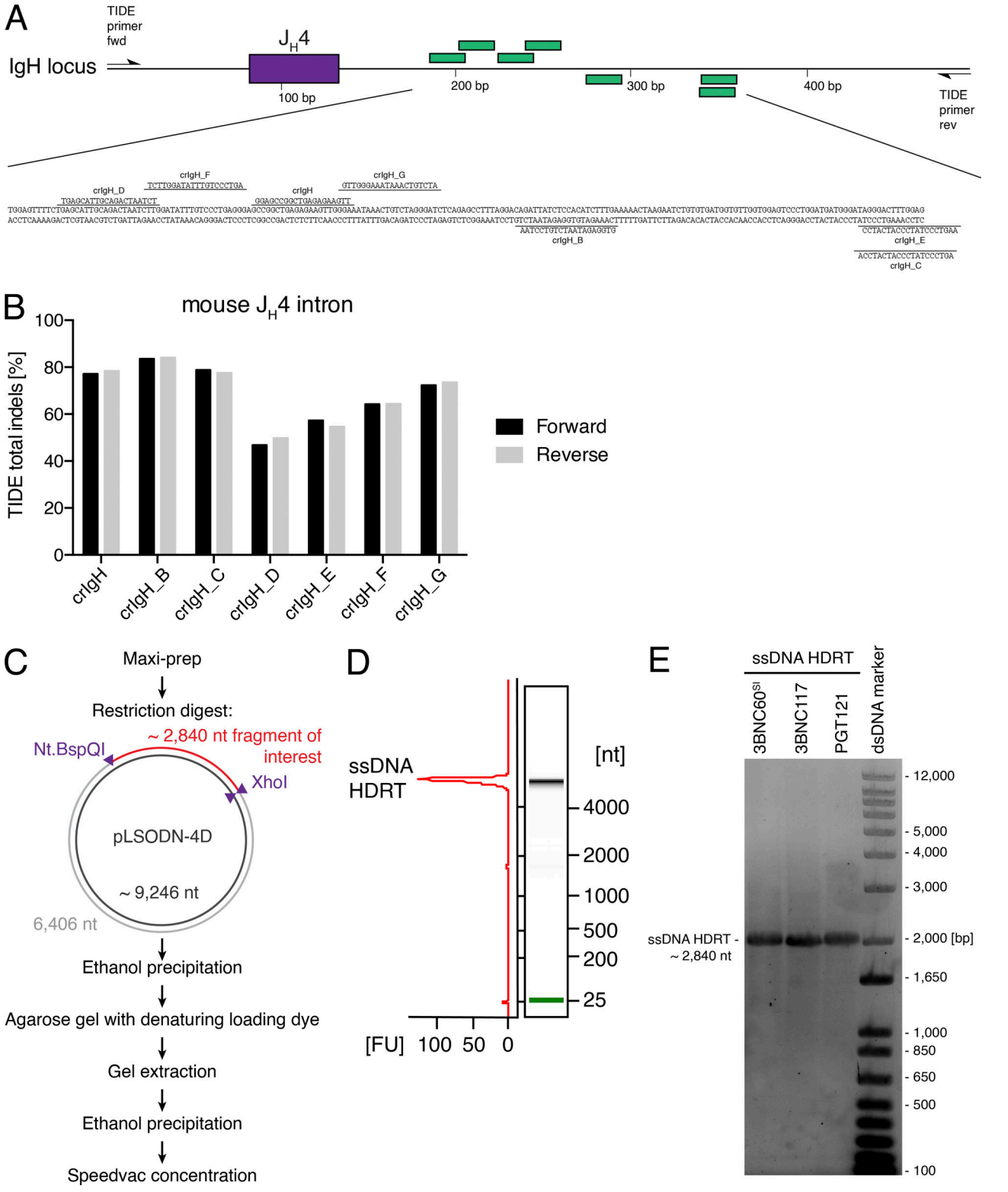

Figure S2. **Identification of optimal mouse *Igh* crRNA and ssDNA HDRT template production. (A)** Schematic representation of the mouse *Igh* locus around J_H4. Location and sequence of tested guide RNAs is indicated below. **(B)** TIDE assay comparing the efficiency of creating indels of the crRNAs indicated in A. Forward (fwd)/reverse (rev) indicate sequencing with forward/reverse primers, respectively. Representative of two independent experiments. **(C)** Flow chart of ssDNA production. HDRT templates were cloned into pLSODN-4D, Maxi-prepared (Maxi prep.), sequence-verified, and digested with restriction enzyme *XhoI* and the nicking endonuclease *Nt.BspQI* to produce three ssDNA fragments of the vector. **(D and E)** Denaturing loading buffer was used to separate the three fragments by conventional agarose gel electrophoresis as indicated. ssDNA HDRT quality and integrity were verified using (D) Bioanalyzer and (E) agarose gel electrophoresis. Representative of >20 independent preparations. FU, fluorescence units.

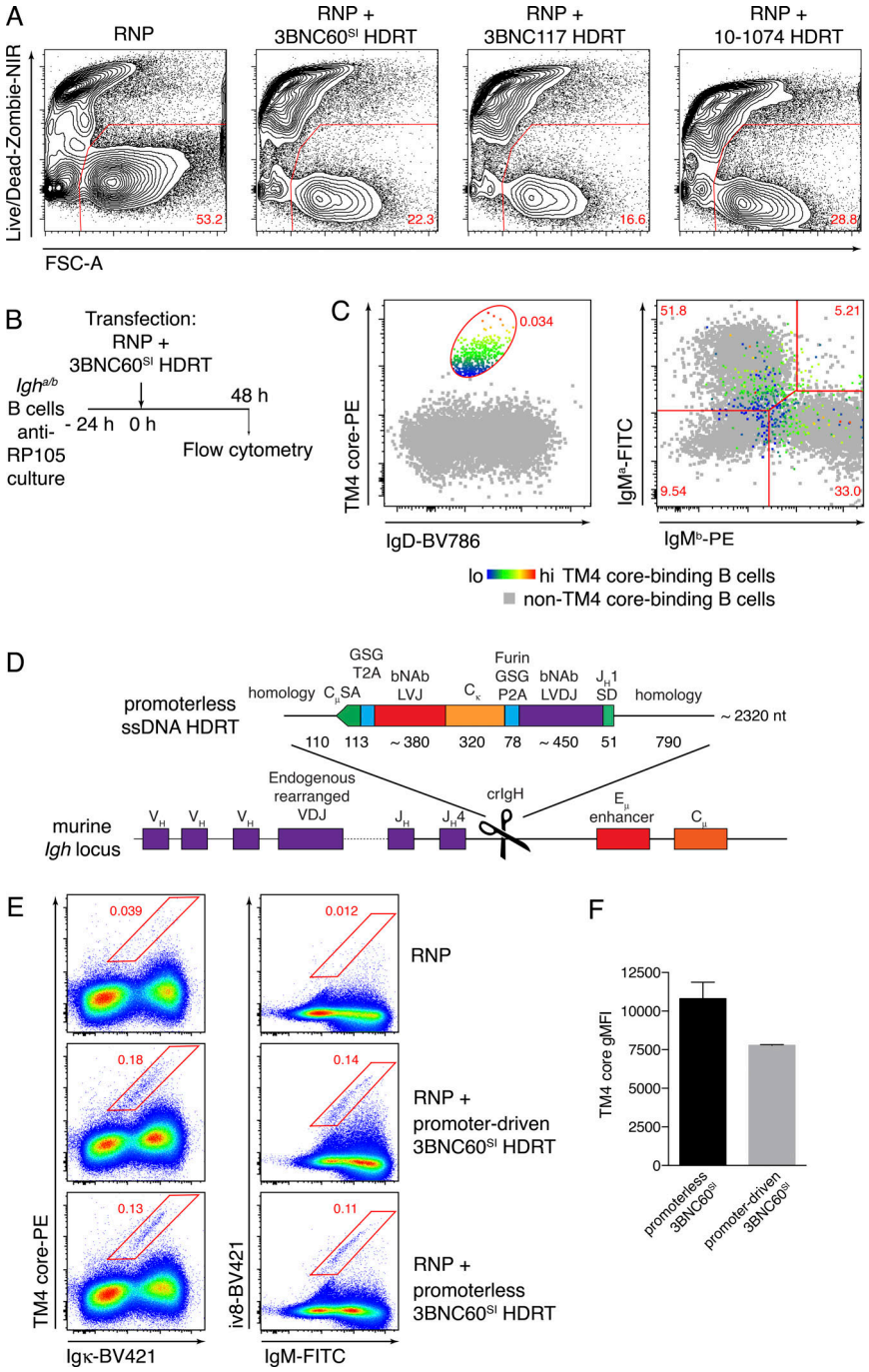

Figure S3. **Cell viability and *Igh* allelic exclusion of bNAb-expressing murine B cells. (A)** Flow-cytometric plots showing percentage of live cells among all events 48 h after RNP ± HDRT transfection. Related to Fig. 2, B and C. NIR, near-infrared dye; FSC-A, forward scatter area. **(B)** Experimental setup for C. Heterozygous ($Igh^{a/b}$) B cells expressing IgH^a or IgH^b alleles were activated for 24 h, then transfected with $3BNC60^{SI}$ HDRT and analyzed 48 h later. **(C)** Overlays of flow-cytometric plots of TM4 core binding cells and nonbinding B cells, both pregated on λ^- B cells. TM4 core mean fluorescence intensity (5.89×10^3 to 1.28×10^5) is color-mapped onto a TM4 core-binding cell population. Numbers represent the percentage of TM4 core-binding cells among λ^- B cells (left) or the percentage of TM4 core-binding B cells in the respective gate (right). Concatenate of five technical repeats in two independent experiments is shown B and C. **(D)** Schematic representation of the promoterless targeting strategy to create bNAb-expressing primary mouse B cells. ssDNA HDRT contained 110 nt 5′ and 790 nt 3′ homology arms flanking an expression cassette. The 5′ homology arm is followed by the 111 nt long splice acceptor site and the first two nucleotides of Cμ exon 1 and an in-frame self-cleaving *Thosea asigna* virus 2A (T2A) sequence with GSG-linker. Then the leader, variable, and joining regions (LVJ) of the respective antibody light chain, and mouse C_κ are followed by a furin-cleavage site, a GSG-linker, and a P2A self-cleaving oligopeptide sequence, the leader, VDJ of the respective antibody heavy chain (LVDJ), and 45 nt of the mouse J_H1 intron splice donor site to splice into downstream constant regions. **(E)** Flow cytometry of mouse B cells transfected and analyzed as in Fig. 2 B either without template, or promoter-driven template or promoterless HDRT encoding $3BNC60^{SI}$. The left panel shows cognate antigen binding (TM4 core), and the right panel identifies correctly edited B cells using anti-idiotypic antibody iv8. **(F)** Geometric mean fluorescence intensity (gMFI) of TM4 core-binding of cells gated as in the left panel of E. Bars indicate mean ± SEM. Representative of two independent experiments.

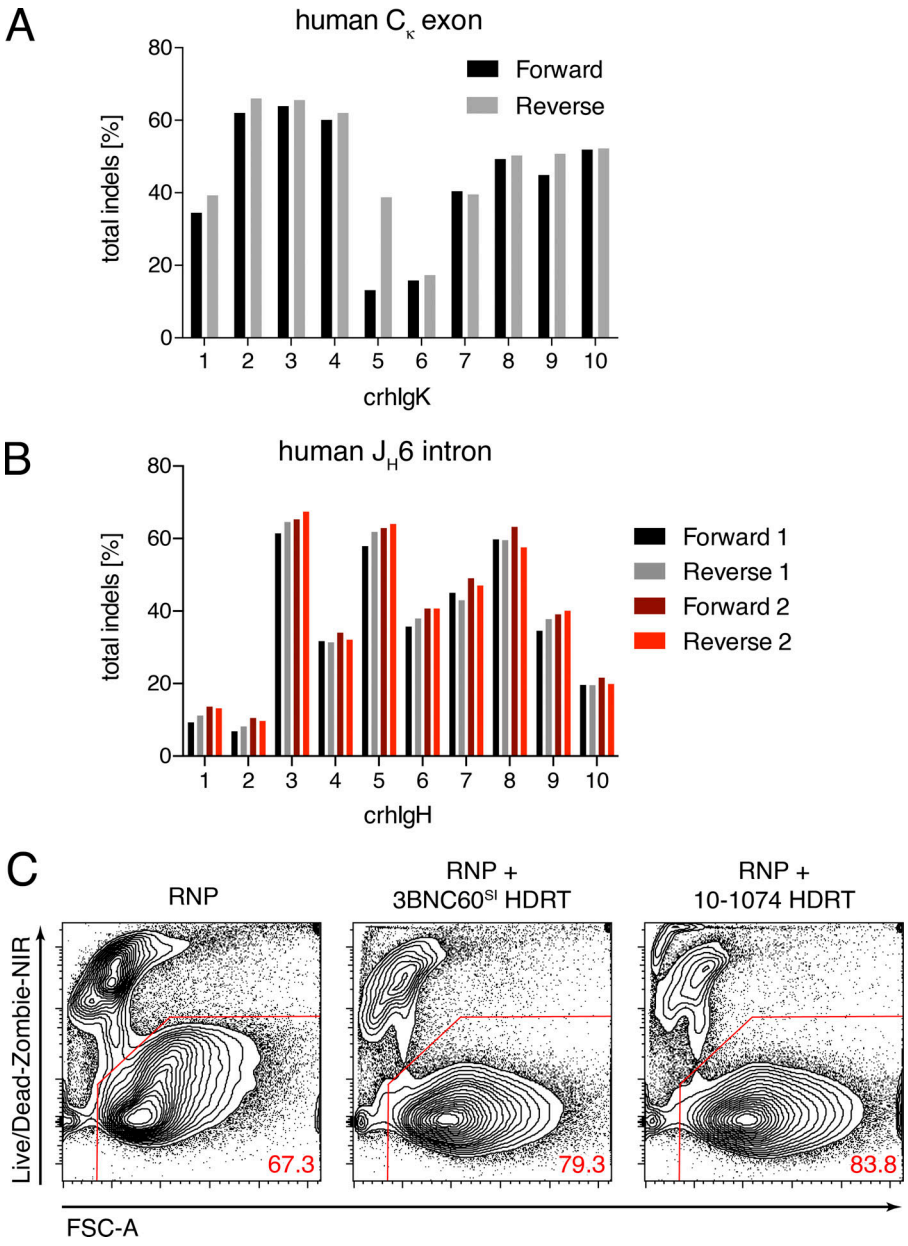

Figure S4. **TIDE analysis and viability of primary human B cells after transfection. (A and B)** TIDE assay 42 h after transfection, comparing the efficiency of creating indels of crRNAs targeting the human *IGKC* exon (A), and TIDE assay using two different primer sets, 24 h after transfection, comparing the efficiency of creating indels of crRNAs targeting the human *IGHJ6* intron (B). Forward/reverse indicate sequencing with forward/reverse primers, respectively. Representative of two independent experiments. **(C)** Flow-cytometric plots showing percentage of live cells among all events 72 h after RNP ± HDRT transfection. Related to Fig. 4 D. Representative plots of two independent experiments are shown.

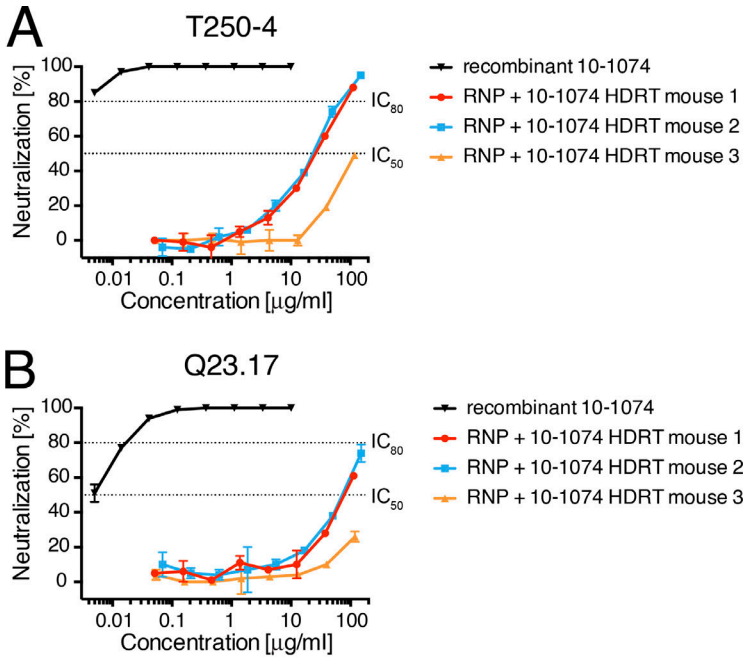

C

Sample	Titer in TZM.bl cells (µg/ml) Virus T247-23 IC_{50}	T247-23 IC_{80}	62357.14.D3.3489 IC_{50}	62357.14.D3.3489 IC_{80}
RNP + 3BNC60^{SI} HDRT mouse 1	>150	>150	>75	>75
RNP + 3BNC60^{SI} HDRT mouse 2	>122	>122	>61	>61
RNP + 3BNC60^{SI} HDRT mouse 3	>61	>61	>61	>61
recombinant 3BNC60SI (µg/ml)	0.390	1.393	0.406	1.946

Figure S5. **Serum neutralization of wild-type mice adoptively transferred with edited B cells.** Related to Fig. 4, A and B. **(A and B)** Neutralization curves for HIV strains T240-4 (A) and Q23.17 (B) of data summarized in Fig. 4 E of mice receiving 10-1074–edited B cells and immunized with cognate antigen 10mut. **(C)** HIV neutralization data of mice receiving 3BNC60^{SI}-edited B cells and immunized with cognate antigen TM4 core. Combined data from two independent experiments (A–C). Curves indicate mean ± SD.

Table S1. **crRNA sequences**

Name	crRNA sequence without PAM	Locus
crIgK$_1$	5′-GTTCAAGAAGCACACGACTG-3′	Mouse *Igkc*
crIgK$_2$	5′-GTTAACTGCTCACTGGATGG-3′	Mouse *Igkc*
crIgH	5′-GGAGCCGGCTGAGAGAAGTT-3′	Mouse J_H4 intron
crIgH_B	5′-GTGGAGATAATCTGTCCTAA-3′	Mouse J_H4 intron
crIgH_C	5′-AGTCCCTATCCCATCATCCA-3′	Mouse J_H4 intron
crIgH_D	5′-TGAGCATTGCAGACTAATCT-3′	Mouse J_H4 intron
crIgH_E	5′-AAGTCCCTATCCCATCATCC-3′	Mouse J_H4 intron
crIgH_F	5′-TCTTGGATATTTGTCCCTGA-3′	Mouse J_H4 intron
crIgH_G	5′-GTTGGGAAATAAACTGTCTA-3′	Mouse J_H4 intron
crhIgK$_1$	5′-GGTGGATAACGCCCTCCAAT-3′	Human *IGKC*
crhIgK$_2$	5′-GTGGATAACGCCCTCCAATC-3′	Human *IGKC*
crhIgK$_3$	5′-CTGGGAGTTACCCGATTGGA-3′	Human *IGKC*
crhIgK$_4$	5′-CCTCCAATCGGGTAACTCCC-3′	Human *IGKC*
crhIgK$_5$	5′-ATCCACCTTCCACTGTACTT-3′	Human *IGKC*
crhIgK$_6$	5′-TTCAACTGCTCATCAGATGG-3′	Human *IGKC*
crhIgK$_7$	5′-GATTTCAACTGCTCATCAGA-3′	Human *IGKC*
crhIgK$_8$	5′-TGGGATAGAAGTTATTCAGC-3′	Human *IGKC*
crhIgK$_9$	5′-ATTCAGCAGGCACACAACAG-3′	Human *IGKC*
crhIgK$_{10}$	5′-GGCCAAAGTACAGTGGAAGG-3′	Human *IGKC*
crhIgH$_1$	5′-GTCCTCGGGGCATGTTCCGA-3′	Human J_H6 intron
crhIgH$_2$	5′-TCCTCGGGGCATGTTCCGAG-3′	Human J_H6 intron
crhIgH$_3$	5′-AGGCATCGGAAAATCCACAG-3′	Human J_H6 intron
crhIgH$_4$	5′-CTCAGGTTGGGTGCGTCTGA-3′	Human J_H6 intron
crhIgH$_5$	5′-ACGAGATGCCTGAACAAACC-3′	Human J_H6 intron
crhIgH$_6$	5′-ACCTGAGTCCCATTTTCCAA-3′	Human J_H6 intron
crhIgH$_7$	5′-TCAGCCATCACTAAGACCCC-3′	Human J_H6 intron
crhIgH$_8$	5′-CAAACCAGGGGTCTTAGTGA-3′	Human J_H6 intron
crhIgH$_9$	5′-CTAAGACCCCTGGTTTGTTC-3′	Human J_H6 intron
crhIgH$_{10}$	5′-TCAGGCATCTCGTCCAAATG-3′	Human J_H6 intron

PAM, protospacer adjacent motif.

Table S3. **Primers for TIDE analysis**

Forward primer 5′ to 3′ sequence	Reverse primer 5′ to 3′ sequence	Comments
5′-CCTGGCCCCATTGTTCCTTA-3′	5′-GCGTCTCAGGACCTTTGTCT-3′	For TIDE analysis mouse *Igkc*, product 483 bp
5′-AATGTCTGAGTTGCCCAGGG-3′	5′-TGTCACAGAGGTGGTCCTGA-3′	For TIDE analysis mouse J_H4 intron, product 495 bp
5′-ATGGCTGCAAAGAGCTCCAA-3′	5′-GGAAAAAGGGTCAGAGGCCA-3′	For TIDE analysis human *IGKC*, product 638 bp
5′-TGCCCTGTGATTATCCGCAA-3′	5′-GAGCTGGAGGACCGCAATAG-3′	For TIDE analysis human *IGKC*, product 515 bp
5′-GCCACTCTAGGGCCTTTGTT-3′	5′-AGCTTCAAGGCACTGAGGTC-3′	For TIDE analysis human J_H6 intron, product 563 bp
5′-CTACATGGACGTCTGGGGC-3′	5′-CTGCTCTCATCAAGACCGGG-3′	For TIDE analysis human J_H6 intron, product 533 bp

Table S4. **Flow-cytometric reagents**

Reagent	Target species	Antibody clone	Company/source	Catalog no.
CD16/32	Mouse	2.4G2	BD Biosciences	7248907
CD4-eF780	Mouse	RM4-5	Thermo Fisher Scientific	47-0042-82
CD8a-eF780	Mouse	53-6.7	Thermo Fisher Scientific	47-0081-82
NK1.1-eF780	Mouse	PK136	Thermo Fisher Scientific	47-5941-82
F4/80-eF780	Mouse	BM8	Thermo Fisher Scientific	47-4801-82
LY6G (Gr1)-eF780	Mouse	RB6-8C5	Thermo Fisher Scientific	47-5931-82
IgG1-APC	Mouse	A85-1	BD Pharmingen	560089
CD95 (FAS)-PE-Cy7	Mouse	Jo2	BD Biosciences	557653
CD45.2-PE	Mouse	104	BioLegend	109808
CD45.1-BV421	Mouse	A20	BioLegend	110732
GL7-FITC	Mouse	GL7	BD Pharmingen	553666
IgD-BV786	Mouse	11-26c.2a	BD Horizon	563618
CD45R/B220-BV605	Mouse/human	RA3-6B2	BioLegend	103244
CD19-PECy7	Mouse	6D5	BioLegend	115520
IgM^a-FITC	Mouse	DS-1	BD Pharmingen	553516
IgM^b-PE	Mouse	AF6-78	BioLegend	406208
Ig light chain λ-APC	Mouse	RML-42	BioLegend	407306
Ig light chain κ-BV421	Mouse	187.1	BD Horizon	562888
IgM Fab-FITC	Mouse	polyclonal	Jackson ImmunoResearch	115-097-020
Zombie NIR	N/A	N/A	BioLegend	423105
Streptavidin-PE	N/A	N/A	BD Pharmingen	554061
Streptavidin-BV421	N/A	N/A	BD Horizon	563259
TM4 core-biotin	N/A	N/A	In house (McGuire et al., 2014)	N/A
10mut-biotin	N/A	N/A	In house (Steichen et al., 2016)	N/A
Anti-$3BNC60^{SI}$ idiotype	N/A	Iv8	In house, this publication	N/A
Human Fc Block	Human	N/A	BD Horizon	564220
Ig light chain λ-APC	Human	MHL38	BioLegend	316609
CD19-PECy7	Human	SJ25C1	BioLegend	363011
IgM-FITC	Human	MHM88	BioLegend	314506
IgD-BV785	Human	IA6-2	BioLegend	348241
Ig light chain κ-BV421	Human	MHK-49	BioLegend	316518

N/A, not available.

Table S2 is provided online as a separate Excel file and lists gBlock sequences of HDRTs.

References

McGuire, A.T., A.M. Dreyer, S. Carbonetti, A. Lippy, J. Glenn, J.F. Scheid, H. Mouquet, and L. Stamatatos. 2014. HIV antibodies. Antigen modification regulates competition of broad and narrow neutralizing HIV antibodies. *Science.* 346:1380–1383. https://doi.org/10.1126/science.1259206

Steichen, J.M., D.W. Kulp, T. Tokatlian, A. Escolano, P. Dosenovic, R.L. Stanfield, L.E. McCoy, G. Ozorowski, X. Hu, O. Kalyuzhniy, et al. 2016. HIV Vaccine Design to Target Germline Precursors of Glycan-Dependent Broadly Neutralizing Antibodies. *Immunity.* 45:483–496. https://doi.org/10.1016/j.immuni.2016.08.016